

See discussions, stats, and author profiles for this publication at: <https://www.researchgate.net/publication/231656402>

Hydrogen Dissociation on Reconstructed ZnO Surfaces

ARTICLE *in* THE JOURNAL OF PHYSICAL CHEMISTRY · MAY 1996

Impact Factor: 2.78 · DOI: 10.1021/jp953704h

CITATIONS

39

READS

12

3 AUTHORS, INCLUDING:



[Lars G M Pettersson](#)

Stockholm University

318 PUBLICATIONS **11,042** CITATIONS

SEE PROFILE

Hydrogen Dissociation on Reconstructed ZnO Surfaces

Mats Nyberg, Martin A. Nygren, and Lars G. M. Pettersson

FYSIKUM, University of Stockholm, Box 6730, S-113 85 Stockholm, Sweden

David H. Gay and Andrew L. Rohl*,†

The Royal Institution, 21 Albemarle Street, London, UK W1X 4BS

Received: December 13, 1995; In Final Form: February 21, 1996®

Atomistic modeling of reconstructions and relaxation of the nonpolar (10 $\bar{1}$ 0) and (11 $\bar{2}$ 0) ZnO surfaces has been performed to obtain more realistic surface structures for embedded cluster quantum chemical calculations of the reactivity of ZnO toward H₂ dissociation. Only small differential geometrical effects are found for the cation and anion top-layer relaxations. Both surfaces are found to be unreactive toward H₂ dissociation. For the polar, Zn-terminated (0001) surface several different reconstructions were studied; the lowest surface energy was obtained for a 4×4 reconstruction containing single-step plateaus and valleys. The highest exothermicity was found for H₂ dissociation over a corner site, involving a low-coordination oxygen, on the plateau. The edge sites on the plateau also lead to exothermic reactions, while the regular sites between plateaus are unreactive. The determining factor for the exothermicity is the coordination of the anion, but the ionization potential at the anion site also shows a correlation with the exothermicity. No cooperative effects were found. The vibrational frequencies were computed in qualitative agreement with experiment for the O–H vibration, while the strong experimental Zn–H peak at 1710 cm^{−1} has not been reproduced. The quantum chemically computed charges on the ions are found to vary with coordination and position; this could have an effect on the atomistic modeling which presently does not include coordination-dependent terms in the potentials. Using an unembedded, gas-phase ZnO unit as a model leads to unrealistically high reaction energies; this is also the case if reconstruction of the (0001) surface is neglected. This demonstrates the need to develop realistic embedding schemes.

Introduction

The surface structure of ZnO prepared by different techniques is of interest in understanding the mechanism of catalytic reactions, such as alkene hydrogenation, alcohol decomposition, and also the water–gas shift reaction where the ZnO plays an important role. ZnO has thus been the subject of a large body of both experimental and theoretical work,^{1,2} but the relationship between structure and reactivity remains somewhat unclear. In addition, the details of the reconstructions and relaxations of the different polar and nonpolar surfaces do not seem to have a satisfactory theoretical explanation.¹

Over the last few years, much work has been devoted to the development of reliable classical two- (or more) body potential descriptions of the interactions between ions in a crystal (for a recent review see, *e.g.*, ref 3) and to the development of efficient computer codes to find minimum energy structures for both the bulk and surfaces. In combination with this, advances in quantum chemical modeling of oxide surfaces enables the direct construction, from the previously atomistically optimized surface unit cell, of properly embedded cluster models^{4,5} for which reactivities toward small test molecules may be studied. Previous studies have concerned the structure and reactivity toward H₂⁴ and H₂O⁵ of the polar Cu⁺-terminated (100) surface of Cu₂O. The relaxation of the surface was shown to lead to a lower reactivity, and it is thus important to include this effect when constructing surface cluster models.

ZnO provides a good case for further studies along these lines, since experimental data are available for, *e.g.*, surface recon-

structions, reactivities of different surfaces, and measured vibrational frequencies for dissociated hydrogen. Furthermore, ZnO is of interest *per se* due to its importance in several catalytic processes as mentioned above. Thus, in the present work we have optimized the surface structures of the nonpolar (10 $\bar{1}$ 0) and the (11 $\bar{2}$ 0) surfaces as well as several different reconstructions of the polar (0001) Zn-terminated surface. As a test for the study of the reactivity associated with each site, we have chosen to use the dissociation of H₂.

The analysis of LEED (low-energy electron diffraction) experiments on the nonpolar (10 $\bar{1}$ 0) and (11 $\bar{2}$ 0) surfaces has led to the conclusion^{1,6} that for the former surface there is a large (0.4 Å) inward relaxation of the top-layer Zn ions, while for the (11 $\bar{2}$ 0) surface there is no relative relaxation of oxygen compared to zinc, and the surface is regarded as an ideal termination of the bulk structure. Theoretical studies have not been able to reproduce both these effects; either no relaxation is found for either surface⁷ or both surfaces are predicted to show large relaxations as in the tight-binding sp³ model of ref 8. In an *ab initio* study of the ZnO (10 $\bar{1}$ 0) surface by Jaffe *et al.*,⁹ the differential relaxation is 0.075–0.115 Å, depending on which method (Hartree–Fock, density functional theory) was used.

For the polar, Zn-terminated (0001) surface an overall 6-fold symmetry is found from LEED.^{10,11} This is quite unexpected, since from only considering the bulk structure, one would expect 3-fold symmetry. This has been explained¹² by assuming a randomly stepped surface with a 60° rotation between adjacent terraces or in terms of hexagonal pits of unknown dimensions.¹³

Since the (0001) surface is polar it must reconstruct or relax to eliminate the dipole across the crystal. Indeed, STM pictures

* Corresponding author.

† Present address: Department of Applied Chemistry, Curtin University, G.P.O. Box U 1987, Perth 6001, Western Australia.

® Abstract published in *Advance ACS Abstracts*, April 15, 1996.

of the (0001) surface show a rough landscape,¹⁴ far from the idealized picture of well-ordered hexagonal pits reported from the LEED experiments. Instead “large” mesas, about 100 Å in diameter, are seen in contrast to the bulklike termination with steps, but with no indication of relaxation, as deduced from angle-scanned photoelectron diffraction studies.¹²

FTIR (Fourier transform infrared) experiments with hydrogen on ZnO surfaces are usually made on powders. Since the (10 $\bar{1}$ 0) surface is the most stable face it is expected to be the most frequently exposed in these experiments. Two main absorption peaks have been assigned to dissociatively adsorbed H₂: the first is the O–H vibration peak at 3510 cm⁻¹, and the second is the Zn–H peak at 1710 cm⁻¹.¹⁵ In addition, a sequence of weaker peaks around 800–1000 cm⁻¹ have been assigned to H or OH bound to more than one ion.¹⁵

Theoretical calculations treating aspects of ZnO surfaces at various levels of theory and sophistication have been reported. Wang and Duke⁸ report on tight-binding calculations including Zn 4sp orbitals in the treatment of (10 $\bar{1}$ 0) and (11 $\bar{2}$ 0) surface relaxation. Jaffe *et al.* have performed periodic Hartree–Fock and DFT calculations on the reconstruction of the (10 $\bar{1}$ 0) surface. Anderson and Jen¹⁶ have employed the semiempirical ASED method to a study of CO oxidation over both the (10 $\bar{1}$ 0) and the oxygen-terminated (000 $\bar{1}$) surfaces using large gas-phase cluster models. Semiempirical MINDO/3 calculations¹⁷ for CO interacting with the Zn polar (0001) surface give a large (0.5 eV) binding energy in agreement with experiment, giving a covalent bond with a strong charge transfer component. The ionicity obtained in the largest Zn₃₂O₃₂ cluster model was quite low (± 0.7) which has been suggested to be due to the limited basis sets used.¹⁸ Hydrogen dissociation over the (10 $\bar{1}$ 0) surface was considered by Nakatsuji and Fukunishi¹⁹ using a ZnO unit either in the gas phase or surrounded by the nearest 32 point charges. These models lead to unrealistically high values for the interaction, due to the neglect of or insufficient treatment of the embedding. Casarin and co-workers^{20,21} have performed local density calculations also using rather large Zn₂₂O₂₂ unembedded cluster models to study the interaction of CO with ZnO. Good results for the CO vibrational shifts were obtained, but the binding energy to the surface was too high, which is an expected result of not including gradient corrections in the functional. Finally, Freitag¹⁸ has performed quantum chemical calculations on the adsorption of CO on the (0001) surface using small (up to Zn₄O₄) cluster models embedded in the Madelung potential. Only weak adsorption was found, and it was suggested that the perfect surface was not representative of the experimental situation and that further reconstructions of the surface should be considered.¹⁸

In the present work we report on results using pair potentials combined with a shell model for the reconstruction and relaxation of ionic models of the above surfaces. In agreement with earlier tight-binding calculations⁷ we find no differential relaxation effects for the nonpolar surfaces. For the polar (0001) surface both 2×2 hexagonal pits and also larger mesas are considered. For each surface model, except for the 8×8 reconstructed (0001), the activity toward hydrogen dissociation was investigated for several different reconstructions and sites and the vibrational frequencies of the resulting adsorbed species were computed. The binding energy was found to be most critically dependent on the anion coordination number, with lower coordination producing a higher interaction. In addition, the most reactive surface was found to be the most unstable, the polar (0001) Zn-terminated surface, in accordance with experiment.

TABLE 1: ZnO Pair-Potential Parameters and Results of Bulk Optimization

1.1. Charges			
	Zn _{core}	Zn _{shell}	O _{core} O _{shell}
q_i	-0.05	2.05	0.00 -2.00
1.2. Buckingham Potentials, $V(r) = A \exp[-r/\rho] - C/r^6$			
	A (eV)	ρ (Å)	C (eV·Å ⁶)
Zn _{shell} – O _{shell}	499.6	0.3595	0.000
O _{shell} – O _{shell}	22764.0	0.1490	27.88
1.3. Core–Shell Harmonic Spring, $V(r) = 1/2 kx^2$			
	k (eV/Å ²)		
O _{core} – O _{shell}	15.52		
Zn _{core} – Zn _{shell}	8.77		
2. Bulk Optimization			
structural parameter	calculated	experiment ^a	
a (Å)	3.2303	3.2495	
c (Å)	5.0767	5.2069	
u	0.389	0.382	
Zn–O distance (Å)	1.948	1.95	
DL spacing (Å)	0.56	0.61	

^a Reference 25.

Methods

The modeling of the surfaces and hydrogen chemisorption on these has been done in two steps: first the reconstruction and relaxation that lead to the lowest surface energy for the particular cut were found, and then a quantum chemical cluster model of relevant sites for the optimized surface structure was constructed. The first step was performed using the program MARVIN,²² which treats surface structure optimizations. This program treats interatomic interactions by two-, three-, and four-body potentials and allows a wide variety of functional forms. All long-range interactions are obtained through proper Ewald summations. The second step uses quantum chemical cluster embedding techniques with a full Ewald summation, based on the relaxed surface unit cell, of the crystal potential contribution to the interaction. We will begin by describing the techniques used to minimize the surface energy for each cut.

The study of the surface reconstructions and relaxations was performed using a pair-potential description of the interactions between the ions in the surface unit cell. In the present application the potentials used for the Zn²⁺–O²⁻ interactions are of Buckingham type. The parameters were optimized²³ for bulk zinc oxide and are given in Table 1 together with the results from optimizing the bulk structure using these parameters. For the bulk-structure optimizations the program GULP²⁴ was used.

As can be seen from Table 1 this description gives results for the bulk that are very close to experiment.²⁵ It should be noted here that the value for the u parameter given by Wyckoff²⁶ is incorrect; the accepted value is 0.382 from X-ray diffraction on a single crystal.²⁵ The lower value given by ref 26 would lead to too large a dipole layer spacing, 0.8 Å compared with the correct value 0.61 Å. The value obtained for c/a is 1.5716, which is only somewhat smaller than the experimental 1.602.²⁶ The accuracy of the pair potentials is deemed quite sufficient for the present investigation.

Having obtained the relaxed structure a quantum chemical model of a reaction site is built up. It is assumed that H₂ will dissociate over a ZnO pair. The cluster models thus include either one, two, or three ZnO units embedded in an environment of total-ion *ab initio* model potentials (AIMP)^{27,28} out to a radius of 13 Å from the cluster with positions determined by the

relaxed surface unit cell. The AIMP descriptions were optimized for Zn^{2+} and O^{2-} ions in the ZnO bulk.²⁹ The Madelung potential was included through a direct evaluation of the Gaussian type integrals over the full Ewald sum^{30–32} generated by the ions in the repeated surface unit cell; this has recently been implemented in the ECPAIMP integral program.³³

The AIMP formalism^{27,28} includes all main quantum mechanical effects of the (frozen) ions making up the environment. Long-range Coulomb interactions are given through the interaction with the ionic charge, and deviations from complete screening are given by a fit in spherically symmetric Gaussians to the potential generated by the actual charge distribution of the ion in the appropriate environment. Core–valence orthogonality is enforced through the use of projection operators built from the ionic core orbitals. Finally, the exchange interaction with the frozen ion is approximated by a spectral resolution of the atomic exchange operator. Thus, for each ion, I , in the environment a term

$$\hat{V}_{\text{Ir-Coul}}^{\text{IMP}}(i) + \hat{V}_{\text{sr-Coul}}^{\text{IMP}}(i) + \hat{V}_{\text{exch}}^{\text{IMP}}(i) + \hat{P}_{\text{proj}}^I(i)$$

is added to the one-electron Hamiltonian. The projection operator term may be written

$$P_{\text{proj}}^I(i) = \alpha \sum_{k \in I} (-2\epsilon_k^I) |\phi_{k,\text{occ}}^I\rangle \langle \phi_{k,\text{occ}}^I|$$

where ϵ_k^I is the orbital energy of the occupied atomic (ion) orbital $\phi_{k,\text{occ}}^I$. α is a scaling parameter, which is set to 0.65 in the present case following ref 34.

The adsorption geometry of one, two, or four hydrogen atoms was finally optimized at the SCF level for each of the cluster models. Binding energies were computed for selected sites also at the MCPF level.³⁵ The basis set for Zn was a small [5s3p2d] contracted basis or a larger [5s4p3d] contraction of Wachters's (13s8p5d) basis³⁶ extended with one or two diffuse p-functions and a diffuse d-function. For oxygen and hydrogen [4s4p1d]³⁴ and [3s1p]³⁷ contracted basis sets were used, respectively.

Results and Discussion

Surface Structures. There are six stable surfaces of ZnO known in the literature. Four of these are nonpolar and two polar with either zinc or oxygen termination. The nonpolar (10 $\bar{1}$ 0) and (11 $\bar{2}$ 0) surfaces show the highest stability, while the higher-order cuts perpendicular to the (401) and (501) directions lead to more unstable surfaces that do not occur in natural crystals.³⁸ The polar (0001) and (000 $\bar{1}$) surfaces are respectively Zn- and O-terminated and are produced from cuts perpendicular to the (001) direction. For the nonpolar cuts it is sufficient to consider relaxation of the ions at the surface, while for the polar surfaces the surface must first be reconstructed to remove the dipole perpendicular to the crystal surface.

An unreconstructed bulk termination of the polar (0001) and (000 $\bar{1}$) surfaces would be electrostatically unstable due to the dipole moment through the crystal. If each layer is assigned a charge density σ , the dipole will be removed if the charge density in the surface layer is decreased by a charge³⁹

$$\sigma' = \sigma \frac{a}{d + a}$$

where a is the interlayer spacing and d is the charge separation within a layer. In the case of ZnO this results in a reduction by approximately 1/4 of the initial surface charge. This can be achieved in several different ways by, e.g., removing

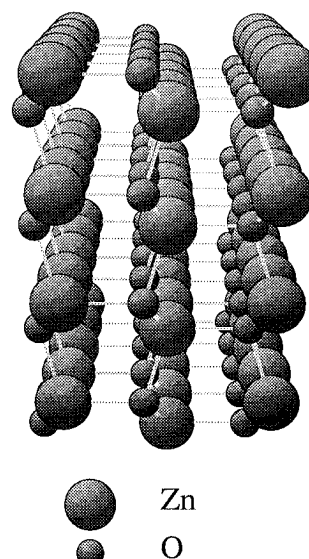


Figure 1. Optimized structure of the (10 $\bar{1}$ 0) shift 1 surface.

some of the ions from the surface, changing the charge of the ions at the surface, or by making regions where the surface is Zn-terminated and other regions which are O-terminated; the latter process may be important in thermal etching where, for the (0001) surface, annealing at 850 K leads to reconstruction of the surface¹⁰ giving local 2×2 and $\sqrt{3} \times \sqrt{3} - 30^\circ$ patches.

In the present work we have chosen to optimize the surface structures by a direct minimization of the total energy of the crystal using a pair-potential approach within the polarizable core shell model. The parameters specifying the potential (Table 1) were optimized to reproduce the bulk structure with an assumed ionicity of ± 2 . These potentials were then applied also in the minimization of the surface energy for the different cuts of the crystal.

Nonpolar Surfaces: (10 $\bar{1}$ 0) and (11 $\bar{2}$ 0). The (10 $\bar{1}$ 0) surface is generated by cutting the crystal perpendicular to the (100) direction in one of two possible ways: either by a cut outside the hexagonal-like unit cell (shift 1) or by cutting the unit cell such that the first layer of ions is removed (shift 2). Both cuts lead to nonpolar surfaces, and thus only relaxation needs to be considered in the structural optimization.

As expected the largest effects of relaxing the surface are found for the top-most atoms. For the shift 1 surface (Figure 1) the top-layer Zn moves downward by 0.22 Å, while the oxygen moves down by 0.26 Å so that very little differential effect on the vertical separation of the cations and anions is found. In addition the ions move toward each other by 0.09 and 0.12 Å for Zn and oxygen, respectively. In the second layer, the effects are smaller and of opposite sign. Thus, the Zn and oxygen move upward by 0.08 and 0.10 Å, respectively. The distortions die off fairly rapidly, and for the third-layer ions the vertical displacements are downward by 0.06 and 0.07 Å, for Zn and oxygen respectively, with an additional lateral displacement of about 0.03 Å each, bringing the ions closer together. The rest of the atoms have very little reconstruction, 0.02 Å or less. The computed surface energy for this surface was 1.1 J/m².

For the shift 2 surface (Figure 2) the motions are somewhat smaller and localized to the two top layers. The Zn ion moves downward by 0.11 Å and moves toward the oxygen by 0.16 Å. Similarly, the oxygen in the top layer moves 0.15 Å downward and toward the Zn by 0.21 Å. The reconstruction is also large for the next layer where the Zn and oxygen move downward

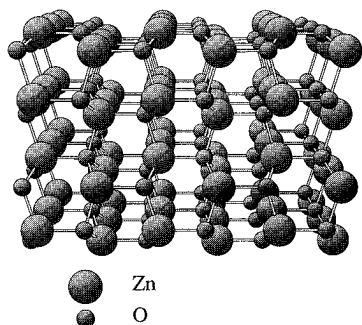


Figure 2. Optimized structure of the $(10\bar{1}0)$ shift 2 surface.

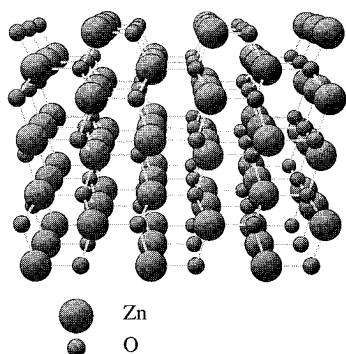


Figure 3. Optimized structure of the $(11\bar{2}0)$ surface.

by 0.13 and 0.15 Å, respectively. The rest of the atoms all show very small movements. This surface was found to be substantially less stable than the $(10\bar{1}0)$ surface, with a surface energy of 3.9 J/m².

The $(11\bar{2}0)$ surface also has a very low surface energy (1.2 J/m²) and is found to relax (Figure 3) in a way similar to what was found for the $(10\bar{1}0)$ surface above. For Zn in the top layer we have a displacement downward by 0.15 Å combined with a motion (0.14 Å) toward the oxygen in the top layer. For oxygen the motions are very similar with a vertical contraction of about 0.17 Å and a side movement of about 0.17 Å. Also in this case only a very small (0.02 Å) vertical differential motion between anions and cations is obtained.

The reconstructions of the nonpolar surfaces have been studied previously both experimentally and theoretically. LEED I-V measurements^{1,6,40} show the $(11\bar{2}0)$ surface to be an ideal bulk termination, while the $(10\bar{1}0)$ surface has been analyzed in terms of an ionic reconstruction with separate contractions of the cation and anion sublattices, where only vertical displacements were considered for the anion lattice. The best fit to the LEED data⁴⁰ was obtained for a contracted top layer with the anions moving downward by 0.10 Å and a larger vertical displacement (-0.30 ± 0.10 Å) for the cations. This is a substantially larger differential effect than that found in the present work.

Wang and Duke⁸ have studied the reconstructions theoretically, using the Zn 4s and O 2p orbitals in a tight-binding model including both nearest- and next-nearest-neighbor interactions. With this model, they obtain only a small (0.043 Å) motion of the O atoms relative to Zn. This is comparable to that which has been obtained in the present work. They also considered a tight-binding sp^3 model also including the Zn 4p orbitals but no next-nearest-neighbor interaction. This gives a very large value for the Zn movement, 0.57 Å, relative to the O atom, which is more in line with what has been deduced from experiment. However, the same model applied to the $(11\bar{2}0)$ surface gave very similar results for the relaxations, with the vertical movement being 0.54 Å in contradiction to what has

been found experimentally. In another theoretical treatment of the $(10\bar{1}0)$ surface by Jaffe *et al.*,⁹ the relative movements of the top Zn and O ions were also investigated, using periodic Hartree–Fock total-energy calculations. Here, the differential effect is much smaller (0.075–0.115 Å). The two top ions move downward toward the bulk on the order of 0.25 Å for the Zn and 0.17 Å for the O ion.

The present approach considers all interactions and motions of the ions in a surface slab which is sufficiently large to reproduce the bulk structure at the interface between the (optimized) surface slab and the (fixed) bulk slab. However, the results will not be better than what is allowed by the potentials used to describe the ion–ion interactions. The present results seem to agree best with the earlier tight-binding calculations omitting the Zn 4p orbitals, and it is interesting to note that for the bulk structure the inclusion of these additional orbitals seems to have only small effects.⁸ The present potentials have been determined from bulk data and could perhaps be improved by considering a modified, less ionic potential for the surface atoms. Additional support for this interpretation will be given in the discussion of the ionicities of the ions in the different models of the surfaces. Ideally one would like to compute the LEED intensities directly from the optimized surface unit cells as an additional test of the reliability of the potentials used and that a structure in agreement with experimental data has been obtained.

Polar Surfaces: (0001) and $(000\bar{1})$. The polar (0001) and $(000\bar{1})$ surfaces in particular must reconstruct, electronically or geometrically, as well as show a relaxation of the surface; the dipole that is generated through the crystal from having a cation or anion termination must be eliminated for a stable surface to be produced. There are several ways that this can be achieved: the stoichiometry at the surface may be altered by moving ions from the top to the bottom of the slab, which for a real crystal would correspond to having ions move to the clef-off crystal side. To eliminate the dipole in the case of the (0001) and $(000\bar{1})$ surfaces of ZnO, one has to remove $1/4$ of the ions at the surface.³⁹ Other possibilities correspond to chemical stabilization by dissociating, *e.g.*, H_2O ,^{41,42} or stabilization by reducing the ionicity of the ions at the surface. Because of the lack of detailed knowledge of the surface structure, workers have normally assumed a bulk termination in the construction of quantum chemical models, *i.e.*, maintaining the bulk stoichiometry and structure also at the surface; in particular for polar surfaces this can lead to serious errors, as will be demonstrated below.

LEED experiments^{10,13} show that there is an overall 6-fold symmetry on the thermally etched surface. This can be interpreted as the surface being stepped, *i.e.*, there are plateaus of different heights which will act to eliminate the dipole. The data have been interpreted¹³ in terms of pyramids, built up by atomic rows. If these are randomly distributed, the 6-fold pattern can be explained (another possibility would be that every Zn ion relaxes to be in the same plane as the oxygens). An estimate of the size of these rows is made in ref 13 with a resulting step height of 6 Å and a width of about three atomic rows. The uncertainties in these figures make the surface difficult to model. STM pictures of the surface,¹⁴ on the other hand, show a very rough landscape with large mesas on the order of 100 Å in diameter.

Several different types of reconstructions were attempted, of which three were able to converge to an energy minimum. In the first, each fourth Zn was removed from the (0001) Zn surface giving a 2×2 surface with vacancies; for charge neutrality an

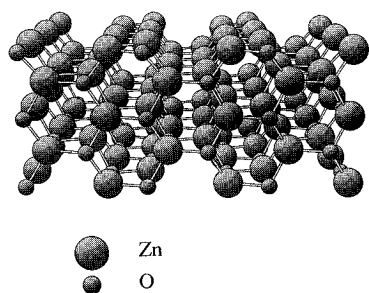


Figure 4. Optimized structure of the 4×4 model of the (0001) surface.

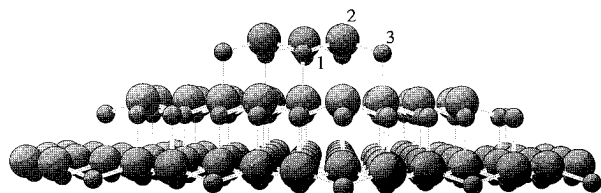


Figure 5. Unrelaxed structure of the 8×8 model of the (0001) surface.

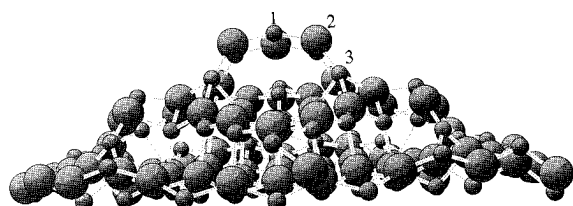


Figure 6. Relaxed structure of the 8×8 model for the (0001) surface.

equal number of oxygen ions was removed from the bottom of the slab. The surface energy for this reconstruction was 2.1 J/m^2 .

A somewhat lower value (1.8 J/m^2) for the surface energy was found for a 4×4 model containing single-step plateaus and valleys. The reconstruction after the cut with this model was very small. The model contains three different regions (Figure 4) where the topmost region is Zn-terminated containing a hexagonal ring of three Zn and three O. The next region is O-terminated and contains only three O, while the third region is again Zn-terminated without vacancies. In optimizing the geometry with MARVIN, the movements of the individual atoms were small and mainly in the z -direction. The largest values were on the order of 0.2 \AA , though the mean displacement was smaller. The Zn:O ratio for the terminating atoms is 4:3, which is not so close to the ideal 3. Experiments on this surface¹² indicate that there is essentially no reconstruction, which could be due to the surface being stepped. This would also explain the observed 6-fold symmetry as due to randomly distributed diatomic step layers;¹² with adjacent planes rotated 60° relative to one another, this would result in an overall 6-fold symmetry.

The third converged model of the surface reconstruction is an 8×8 model. The result is a complicated structure, see Figures 5 and 6, with substantial rearrangements of the ions. The six top-layer atoms (1 and 2 in Figure 6) form an almost hexagonal ring, which is about 3.1 \AA above the next layer. These six atoms are all three-coordinated. The oxygen atoms that once were in the top layer, belonging to the edge site (number 3 in Figure 6), have moved closer to the second-layer atoms and are now four-coordinated instead of the original coordination number of 2. The absolute 6-fold symmetry at the atomic level becomes broken, in that the top ring, for instance, is not exactly hexagonal, but the model still has a hexagonal translational symmetry of the regions. The rearrangement is much larger than in the 4×4 case; the resulting surface energy is surprisingly

high, 2.5 J/m^2 , considering the experimental observation of rather large mesas. Thus we have not found a smooth convergence of the surface energy as we investigate larger and larger models of "mesa"-like structures.

Hydrogen Dissociation

The dissociation of H_2 was assumed to occur heterolytically over neighboring Zn and O ions. Only the final state of the reaction was investigated, *i.e.*, the binding energy of two hydrogen atoms on neighboring sites of the surface was compared to that of H_2 ($D_e = 4.577 \text{ eV}$ at the MCPF level using the present basis sets and 4.751 eV experimentally⁴³). The results are presented in Tables 2 and 3 and will be discussed for the different surfaces and cluster models below.

Nonpolar Surfaces: $(10\bar{1}0)$ and $(11\bar{2}0)$. The most stable relaxed $(10\bar{1}0)$ surface from the simulation was the shift 1 cut which was taken to represent the surface. The simplest model one can assume is a single gas-phase ZnO unit, which has previously been used as a model of this surface by Nakatsuji *et al.*¹⁹ We will begin by discussing the results of this very simple model and then continue with embedding the ZnO unit to see the effects of the crystal surrounding.

Taking a single gas-phase ZnO unit as a model allows one to perform complete geometry optimizations without having to consider the additional complication of the gradients with respect to the embedding Hamiltonian. Using the present basis sets the optimized (SCF) free ZnO distance becomes 1.76 \AA , which is reasonably close to the value (1.95 \AA) in the ZnO bulk. The state considered was the singlet state, even though the triplet state for gas-phase ZnO is the ground state,⁴³ since the singlet state becomes stabilized in the matrix.⁴⁴ The intrinsic bonding is quite ionic with charges of ± 1.97 according to the Mulliken population analysis.

A full geometry optimization of the $\text{ZnO} + \text{H}_2$ system leads to an almost linear molecule, with the hydrogens at the ends. This situation could not occur on the surface, since there are Zn or O too close to the positions of the hydrogens. Instead of using this optimized system, the hydrogens were placed directly above the Zn and O, perpendicular to the Zn–O axis, and a restricted geometry optimization was performed. The optimized distances were 0.935 and 1.66 \AA for the O–H and Zn–H bonds, respectively, with associated vibrational frequencies of 4018 cm^{-1} (O–H) and 1540 cm^{-1} (Zn–O) in good agreement with experiment. The binding energy, however, becomes extremely large (5 eV) so that it is unlikely that the model is relevant for the description of the energetics of hydrogen dissociation on the $(10\bar{1}0)$ surface; note that embedding the ZnO unit leads to substantially smaller interaction energies (see below).

The dissociation of H_2 on ZnO has been described¹⁹ through an electron donation from the $2p\pi$ orbital of O to the antibonding σ_u^* MO of H_2 and a back-donation from the bonding σ_g MO of H_2 to the LUMO of ZnO. This picture is substantiated in the present calculations where the transfer seems to be mainly from O($2p$) to H($1s$). The main effect of the electrostatic embedding will be to modify the amount of charge transfer.

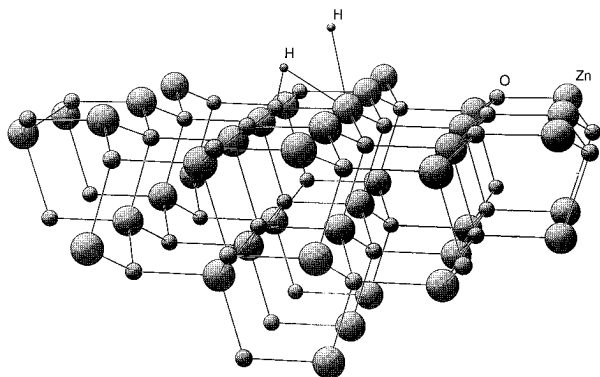
The small $(10\bar{1}0)$ model consists of 1 Zn, 1 O, and 2 hydrogens, embedded in an immediate surrounding consisting of 20 Zn^{2+} and 20 O^{2-} ions represented by total ion AIMP. This is further embedded in a large number of point charges, placed in the atomic positions of the relaxed crystal. The model with hydrogens in the optimized positions is seen in Figure 7. The hydrogen dissociation is found to be endothermic by 0.34 eV so that this surface model will not dissociate H_2 . Inclusion of correlation through an MCPF treatment only leads to a more endothermic reaction. Extending the model to include the two

TABLE 2: Computed Exothermicities (eV) for Hydrogen Dissociation at Different Sites of the Surfaces Studied. SCF and MCPF Results

surface	model	site	coordination		SCF	MCPF
			Zn	O		
Nonpolar Surface						
(10 $\bar{1}$ 0)	small		3	3	-0.34	-0.42
(10 $\bar{1}$ 0)	large		3	3	-1.0	
(11 $\bar{2}$ 0)		parallel	3	3	-0.03	-0.10
(11 $\bar{2}$ 0)		orthogonal	3	3	-0.19	-0.22
(11 $\bar{2}$ 0)	large	parallel	3	3	-0.20	
(11 $\bar{2}$ 0)	large	orthogonal	3	3	-0.50	
(11 $\bar{2}$ 0)	large	four hydrogens	3	3	-0.11 (*2)	
Defect						
(11 $\bar{2}$ 0)	O(2-) vacancy		2	3	4.33	
Polar Surface						
(0001)	bulk		3	3	4.47	
(0001)	2×2	near hole	3	2	0.63	0.32
(0001)	2×2	not near hole	3	3	-1	-0.93
(0001)	4×4	corner	3	2	1.07	0.85
(0001)	4×4	edge	3	3	0.57	0.26
(0001)	4×4	terrace	3	4	no bonding	
(0001)	4×4 large	corner	3	2	1.30	1.16
(0001)	4×4 large	edge	3	3	0.26	0.33
(000 $\bar{1}$)	4×4	corner	2	3	-0.16	
(000 $\bar{1}$)	4×4	edge	3	3	-0.88	

TABLE 3: Mulliken Population Charges for Systems with Hydrogen. Values for the Naked Cluster in Parentheses

surface	model	site	Zn	O	H(ZnH)	H(OH)
(10 $\bar{1}$ 0)	small		+1.59(1.54)	-1.25(-1.54)	-0.67	+0.33
(11 $\bar{2}$ 0)		parallel	+1.62(1.59)	-1.28(-1.59)	-0.63	+0.30
(11 $\bar{2}$ 0)		orthogonal	+1.67(1.59)	-1.24(-1.59)	-0.66	+0.24
(0001)	bulk		+0.77(0.69)	-0.85(-0.69)	+0.27	-0.19
(0001)	2×2	near hole	+1.70(1.50)	-1.14(-1.50)	-0.80	+0.25
(0001)	2×2	not near hole	+1.71(1.59)	-1.17(-1.59)	-0.76	+0.21
(0001)	4×4	corner	+1.55(1.50)	-1.15(-1.50)	-0.67	+0.27
(0001)	4×4	edge	+1.72(2.02)	-1.19(-2.02)	-0.76	+0.23
(0001)	4×4	terrace	+1.45(1.57)	-1.18(-1.57)	-0.56	+0.29
(0001)	4×4 large	corner	+1.65(1.53)	-1.12(-1.53)	-0.81	+0.15
(0001)	4×4 large	edge	+1.90(1.86)	-1.16(-1.86)	-0.80	+0.17

**Figure 7.** Optimized structure of hydrogen on the (10 $\bar{1}$ 0) surface.

nearest Zn and O at the all-electron level also gives a much lower reaction energy (-1.0 eV).

In the optimized structure the H-H distance is 1.59 Å or about twice that of free hydrogen gas. A second minimum was found with an even longer H-H distance (1.75 Å), but still with the same binding energy. The bonding can be characterized by a charge transfer from one hydrogen to the other. The oxygen donates some charge to the hydrogen attached to the Zn, and the hydrogen on O also acts as a donor. The Zn atom seems rather passive in this reaction.

The ionicities of the Zn and O ions in the larger (Zn₃O₃) model are somewhat different from those in the small model (Table 3). This is because in the small model, the electrons are restricted to the two atoms in the cluster, while in the larger

model they are distributed without restrictions on the six atoms in the cluster; the resulting charge distribution is quite site-dependent.

The present results are strongly at variance with the results obtained by Nakatsuji and Fukunishi¹⁹ in their theoretical study of H₂ on ZnO(10 $\bar{1}$ 0). They use a single ZnO unit, first without any surroundings at all and then with the nearest 32 point charges. They obtain vibrational frequencies quite close to the experimental ones (4090 and 1730 cm⁻¹), and a very large binding energy for the system, 3.5 and 3.2 eV for their respective models. In comparing the present results with those of ref 19 it seems clear that the discrepancy is due to an insufficient treatment in ref 19 of the electrostatic interaction and the Pauli repulsion to the nearest neighbors. Their results are quite close to the gas-phase ZnO model and would be interpreted to indicate a highly reactive (10 $\bar{1}$ 0) surface, in contradiction with experiment.

The (11 $\bar{2}$ 0) surface was modeled by a ZnO unit embedded using the same approach as for the (10 $\bar{1}$ 0) surface above. Hydrogen dissociation was considered over two different sites, and the resulting optimized structures are shown in Figure 8. Neither of the sites leads to an exothermic reaction with H₂, and the conclusion is that a low reactivity should be expected also for this surface; this is true both with and without dynamical correlation.

The Polar (0001) Surface. A model of the unreconstructed bulk-terminated (0001) surface was first set up as an illustration of the Madelung instability and the necessity to take reconstruction and relaxation into account. Thus, a single ZnO unit was

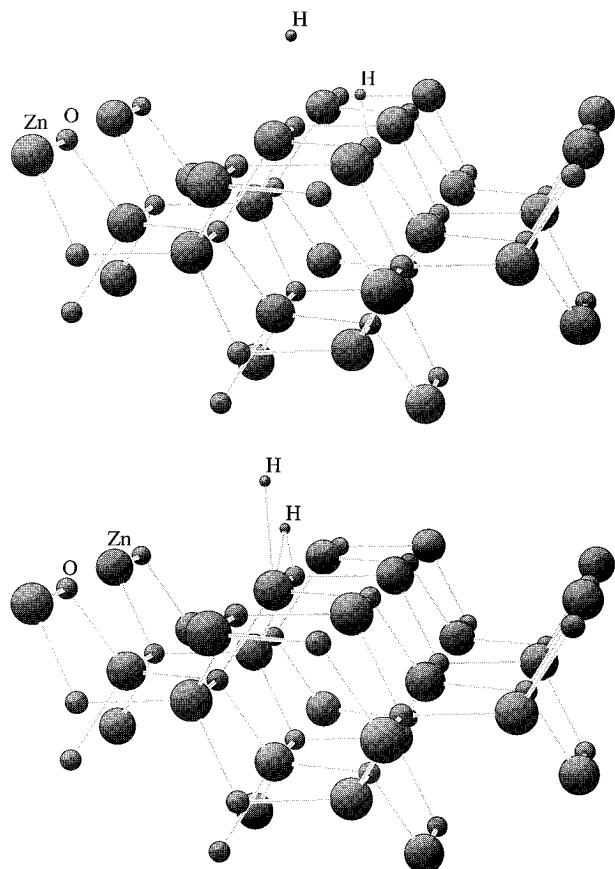


Figure 8. Optimized geometries of (a, top) the orthogonal and (b, bottom) the parallel site of the (1120) surface.

embedded in a set of ECPs and point charges representing the unreconstructed surface and the hydrogen chemisorption energy were computed for this model. The result is an extremely high exothermicity of 4.47 eV; this is due to the intrinsic instability of the surface. Thus, the bulk-terminated unreconstructed (0001) surface cluster model is not a valid representation of the physical situation and reconstruction, either geometrical or electronic (as in, *e.g.*, ref 18), must be taken into account to remove the dipole across the crystal.

2×2 Surface with Vacancies. Assuming that the dissociation takes place over a Zn–O pair of ions acting as a Lewis acid–base site there are two sites of particular interest on this surface. One is the site near a vacancy, and the other is a fully (surface) coordinated Zn–O pair. A larger reactivity is expected for the pair near the vacancy than for the pair with higher oxygen coordination number. This is also the result of the calculations where a binding energy of 0.63 eV relative to gas-phase H₂ is obtained for the low-coordination site, while the reaction is endothermic by 0.98 eV for the saturated site away from the vacancy; at the MCPF level the corresponding values are 0.32 and −0.93 eV, respectively. For the saturated site, the lowest energy found was for both of the hydrogens on top of the oxygen atom, while for the model near the vacancy, the minimum was obtained for one H on Zn and the other on O.

Terraced 4×4 Surface. Three different sites on the terraced 4×4 surface have been investigated: Two of these are on the hill, and one is on the lower step (Figure 9); the strongest bonding is expected to occur at the low-coordinated corner. Since the site on the lower step has more nearest neighbors, this site is expected to be fairly unreactive. At the SCF level no bound states were found for hydrogen on the two highest-coordinated sites, while at the corner, where the outermost oxygen atom has only two neighbors, the bonding energy is

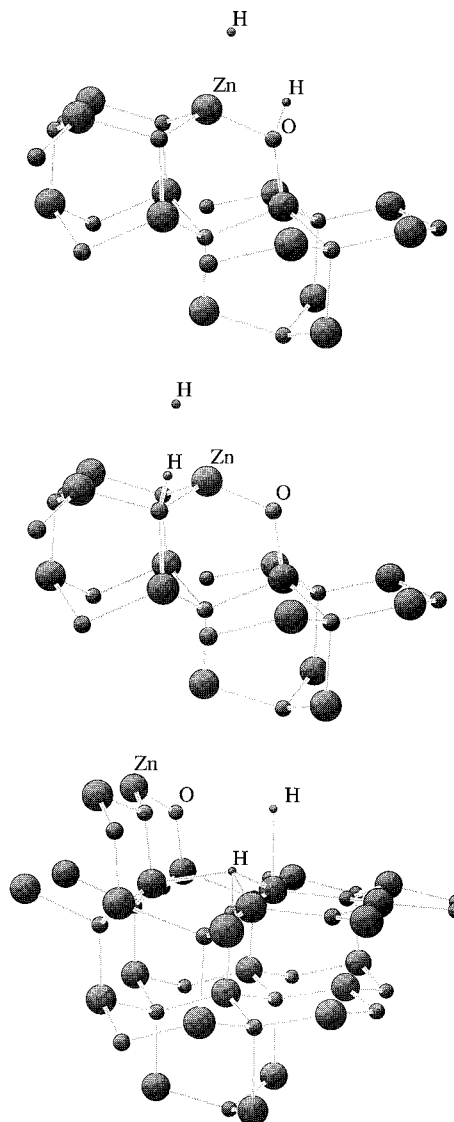


Figure 9. Optimized geometries of the hydrogens adsorbed on the 4×4 model of the (0001) surface: (a, top) corner site, (b, middle) edge site, and (c, bottom) lower terrace site.

1.07 eV (MCPF: 0.85 eV). The second site on the terrace edge gave a binding energy of 0.57 eV (MCPF: 0.26 eV). Finally, for the site on the lower terrace, no bound state was found. Only on-top sites have been considered for the lower terrace, *i.e.*, sites where the hydrogens are directly above Zn and O. Although a full geometry optimization has not been performed, the endothermicity of 3.3 eV makes it very likely that this is an unreactive site. Thus, the low-coordinated corner site is the most reactive while the bottom site, with the highest coordination, is the least reactive site.

Cooperative effects in the dissociation of H₂ on MgO have been reported by Morokuma and co-workers.⁴⁵ They suggest an electrostatically controlled mechanism, based on the rock-salt structure of the MgO crystal. With a heterolytic dissociation resulting in a negative charge on the hydrogen associated with Mg²⁺ and a positive charge with that associated with O^{2−}, they suggest that the electric field induced by the charged hydrogens should facilitate and stabilize the charge rearrangement within the second H₂ unit. Indeed, from a model based on replacing the first pair of hydrogens by appropriate point charges, most of the cooperative effect is recovered.⁴⁵ The charge distributions given in Table 3 for H₂ on ZnO show that also in the present case the heterolytic dissociation process is operative; the

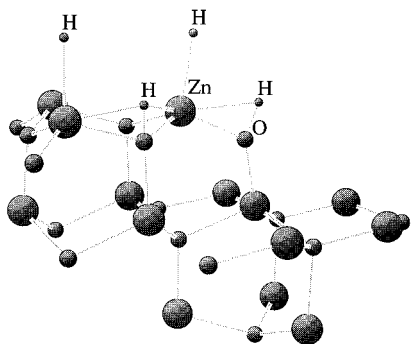


Figure 10. 4×4 model of the (0001) surface with four hydrogens adsorbed.

hydrogen associated with Zn becomes negatively charged while charge is transferred from the hydrogen of the OH group.

In the present case, however, except for the trivial case of two hydrogen atoms, no cooperative effects have been found. In atomic chemisorption, the chemisorption energy of the first hydrogen, either on the Zn or on the O, is always less than half the chemisorption energy for the pair of hydrogen atoms. This may be viewed as the first hydrogen atom forming a covalent bond to the surface, leading to the breaking of the bond between the Zn–O pair, or alternatively in an electrostatic picture, as the first hydrogen generating a stabilizing field that facilitates the charge transfer for the second hydrogen. However, for dissociative chemisorption of more than a pair of hydrogens neither of these effects seem to be operative and the net effect found is a repulsion with the first pair of hydrogens.

The existence of cooperative effects in the hydrogen dissociation was investigated using a larger embedded $(\text{ZnO})_2$ model of the terrace edge and corner (Figure 10). The binding energy of four hydrogens to the cluster model was computed and compared with the energy computed for one pair of hydrogens at a time. The geometry was fully optimized for each of the two sites separately, and the optimized geometry was then used for the composite system, *i.e.*, with four hydrogens. For the corner site, with a two-coordinated oxygen, the exothermicity was separately computed to be 1.30 eV, while for the edge site, where both Zn and O are three-coordinated, an exothermicity of only 0.26 eV was found. For the combined system, however, the reaction at this geometry was found to be endothermic by 1 eV compared to two H_2 molecules. This is an upper bound on the endothermicity since the geometry was not reoptimized for the combined system but instead taken as the separately optimized geometries. However, it is unlikely that more than 2.5 eV (which would be required to give a net positive contribution from the presence of the other pair of hydrogens) could be recovered from a further geometry optimization and no cooperative effect is thus found at this surface. For the (11 $\bar{2}$ 0) surface a small cooperative effect was found but not sufficient to make the process exothermic.

Since the process of H_2 dissociation on ZnO is mainly a donation of electrons from O2p to H, a higher binding energy could be expected at sites where the O2p IP is low. In Figure 11 we show a graph of the Koopmans' values for the IP of the different embedded cluster models and compare that with the computed exothermicities in the H_2 dissociation. It is clear that, although the spread is rather large, the ionization potential at the surface site is of importance in determining the exothermicity. This also leads to an expected dependency on the exact value of the embedding electrostatic potential.^{46,47}

A true value of the charge of the ions in the bulk crystal is difficult to establish. Different experimental techniques give results covering the range from ± 0.4 from Phillip's ionicities

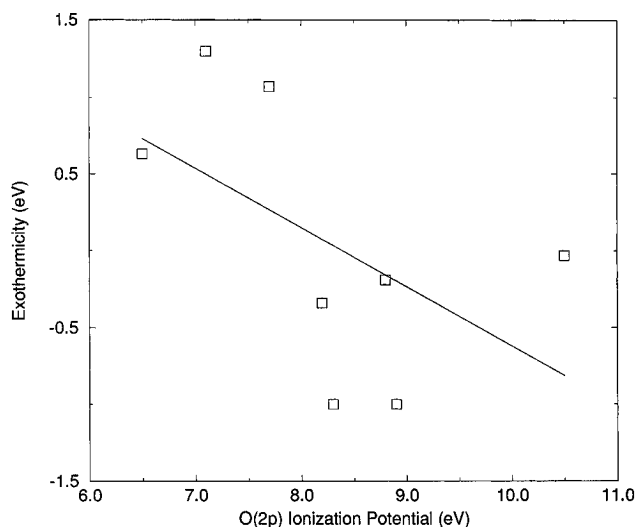


Figure 11. Exothermicity in the H_2 adsorption compared to the Koopmans's values for the O(2s) ionization potential.

to ± 1.1 –1.7 from XPS data.² Quantum chemical models tend to give higher values, *e.g.*, ± 1.8 as reported by Siegbahn and co-workers⁴⁴ from a self-consistent optimization of the embedding charges. Furthermore, the charges at the surface cannot be expected to be the same as in the bulk. Indeed, in the cluster models we do see a variation of the ionicities with the position of the ion relative to the surface. This is illustrated by the 4×4 terrace model of the (0001) surface, where both the corner and edge sites were studied separately and jointly. For the small model consisting of a single embedded ZnO unit the Mulliken charges were found to be ± 1.5 and ± 2.0 for the corner and edge sites, respectively. In the $(\text{ZnO})_2$ model, where both sites are included, the charge distribution was found to be -1.7 for each of the oxygens, while the Zn charges were obtained as $+1.5$ for the corner site and $+1.9$ for the edge site. Thus, even though the absolute values of the Mulliken populations cannot be given strict significance, we must conclude that ions at differently coordinated and exposed sites at the surface must be assumed to have a variable ionicity and possibly different amounts of covalent character in their interactions, *i.e.*, different occupation of the 4sp states in the case of Zn.

Since the ionicity depends on the structure and the position of the ions, an uncertainty is introduced in the structure simulation. This makes modeling the surface with a program like MARVIN somewhat arbitrary in the sense that choosing a charge, for instance ± 2 , may also affect the resulting structure of the surface. As a simple test of the sensitivity of the structure to the assumed value of the ionicity we have reoptimized the (10 $\bar{1}$ 0) surface for a charge of ± 1.8 ; the potential will no longer be consistently determined, but for small changes in the ionicity we may assume that the main effects will be due to the modified charge. The result was an increase in the *c*-parameter by approximately 0.1 Å. No large change for *a* was seen. The surface structure, however, is very similar to that obtained using the higher charge. The overall difference is only a larger value for interatomic distances. The relaxation of the top layer atoms, however, becomes smaller in magnitude for the lower value of *q*. A value for the top Zn is 0.14 Å and for the top O 0.16 Å. Still there is a discrepancy compared to the experimental values in that there is a larger relaxation for the O atom than the Zn.

Although the structure may be sensitive to the ionicity, the properties of the embedded cluster are not expected to be very dependent on the assumed ionicity once the cluster is large enough. In the present case we believe the determining factor for the reactivity is the effective coordination number of the

TABLE 4: Computed SCF-Level Vibrational Zn–H and O–H Frequencies (cm⁻¹) for Different Surfaces and Sites. Scaled Values in Parentheses (See Text)

surface	model	site	$\omega_e(\text{ZnH})$	$\omega_e(\text{OH})$
gas phase				
(1010)	small		1083 (984)	3296 (2996)
(1010)	large		1115 (1014)	2891 (2628)
(1120)	para		1057 (961)	3735 (3395)
(1120)	ortho		1034 (940)	3501 (3183)
(1120)	O(2-) vacancy		1709 (1554)	3860 (3509)
(1120)	O vacancy		1456 (1324)	
(0001)	2×2	near hole	784 (713)	2573 (2339)
(0001)	4×4	corner	1232 (1120)	4050 (3682)
(0001)	4×4	edge	1215 (1104)	3595 (3268)
(0001)	corner		1476 (1342)	3888 (3534)
(0001)	edge		1166 (1060)	4055 (3686)
expt ^a			1710	3510

^a Reference 15.

individual atoms, which in turn depends on the relaxation. In many theoretical calculations on surface properties, the relaxation has been ignored; although there are uncertainties associated with the potentials used in MARVIN, the present and previous⁴ work demonstrate that relaxation has important effects on the properties and should thus be considered in the model.

Vibrational Frequencies

The vibrational frequencies were evaluated for each of the hydrogen atoms separately using displacements of 0.03 Å and considering both Zn and O as fixed at the surface. The results were obtained at the SCF level, which is known to result in frequencies that are approximately 10% too high and thus we report in Table 4 both the directly computed values and the results after scaling.

The experimental FT-IR spectrum¹⁵ shows three groups of absorption peaks that have been assigned to $\nu(\text{O–H})$ (3385–3495 cm⁻¹), $\nu(\text{Zn–H})$ (1480–1753 cm⁻¹), and $\delta(\text{O–H})$, $\delta(\text{Zn–H})$, $\gamma(\text{O–H})$ and more complex interactions in the region of 640–950 cm⁻¹. The measurements were performed on powder samples and should thus represent the most stable faces of ZnO, *i.e.*, the (1010) and the (1120) faces. The computed frequencies should be regarded as qualitative since the models are small and the effects of correlation only estimated through the scaling of the SCF results. However, it is clear that the O–H absorptions are more easily reproduced in the calculations than the absorptions assigned to Zn–H. In fact, for the nonpolar surfaces no Zn–H vibrations are in the region experimentally assigned as the Zn–H vibration. This could imply that the sites considered in this work are not the ones responsible for hydrogen dissociation or that the Zn–H vibrations seen experimentally stem from vacancies or other defects and the peaks in the lower region are due to dissociation on regular sites. In fact, using a simple model of an anion vacancy with either an O²⁻ (leading to a charged defect) or a neutral oxygen removed leads to a higher Zn–H frequency in the neighborhood of the experimental value (Table 4). The intensity of the peak at 1710 cm⁻¹ is, however, so large that regular sites are probable. This problem will be addressed in future work.

Conclusions

Atomistic simulations and quantum chemical cluster modeling have been combined to give a more comprehensive treatment of structure and reactivity of metal oxide surfaces. All surfaces must relax to some extent relative to the bulk structure, which leads to a stabilization of the surface and consequently to a lower reactivity. In particular for the polar surfaces the dipole through

the crystal must be eliminated to produce a stable surface; this can be achieved through geometrical reconstructions where a fraction of the majority species at the surface is moved to the opposite crystal face or through, *e.g.*, an electronic stabilization. In the latter case the ionicity of the ions at the surface would be reduced so as to eliminate the dipole. The present work has been focused on the effects of geometrical relaxations using the same interaction potentials for all ion positions, *i.e.*, in the bulk and at the surface. This is an approximation and should be followed by an investigation of the effects of varying the description depending on the coordination of the ions. In fact, in the larger cluster models employed in the present work, different Mulliken charges were found for cations in different sites near the surface. These charges must be regarded as only qualitative but may still indicate that the interionic potentials could be modified to take this effect into account. The dominant effects of the interactions, both at the surface and in the bulk, are believed to be already included in the present description, however.

Relatively large motions of the ions in the surface layers were found. In particular for the (1010) and (1120) surfaces earlier LEED data indicate a large differential inward relaxation of the Zn ions in the former case, while the (1120) surface is regarded as an ideal bulk termination. In the present investigation no differential effect is found for either surface, which is in agreement with earlier tight-binding calculations but in disagreement with more extended calculations including also the Zn 4p orbitals. In the latter case, large differential relaxation effects were found for both surfaces so that a satisfactory theoretical treatment of these surfaces does not seem to be available. *Ab initio* calculation⁹ on the (1010) surface give a smaller differential relaxation for the topmost atoms than these tight-binding calculations including 4p orbitals, but also here, the Zn ion relaxation is larger. A reinvestigation of the LEED data taking into account a more extended set of parameters and also the present energy-optimized surface unit cells would be of value to resolve this discrepancy.

The polar (0001) Zn-terminated surface shows larger relaxations, in particular when terraces, steps, and mesas at the surface are considered. This is also the only surface that, in the present investigation and also experimentally, shows significant reactivity toward H₂ dissociation. The exothermicity is strongly correlated with the coordination of the ions, with the highest reactivity found for a corner site of a 4×4 plateau at the reconstructed surface. The edge site, where both Zn and oxygen are three-coordinated, also gives an exothermic reaction with H₂, but the regular sites on the terraces between plateaus are found to be unreactive. No cooperative effects between adsorbates were found for any of the investigated sites.

Small cluster models that do not include the embedding, *e.g.*, a single gas-phase ZnO unit, or an insufficient treatment of the embedding, either through too few point charges or through not taking charge reconstruction into account in the case of polar surfaces, are shown to lead to erroneous results with strongly exaggerated binding energies. For larger cluster models, such as employed in some previous semiempirical studies, the effects of the embedding (external to the cluster) can be expected to be diminished and as a further check of the embedding scheme used in the present study it will be of importance to treat much larger cluster models at the present high level of theory. In particular, for the identification of the site responsible for the Zn–H vibrational frequency obtained experimentally more work will be needed.

Acknowledgment. This work was partly supported by funds from the Swedish Consortium on Oxidic Overlayers. D.H.G.

would like to thank BIOSYM Technologies, San Diego, for their financial support.

References and Notes

- (1) Henrich, V. E.; Cox, P. A. *The Surface Science of Metal Oxides*; Cambridge University Press: Cambridge, 1994.
- (2) Kung, H. H. *Transition Metal Oxides: Surface Chemistry and Catalysis*; Elsevier: Amsterdam, 1991.
- (3) Catlow, C. R. A.; Bell, R. G.; Gale, J. D. *J. Mater. Chem.* **1994**, *4*, 781.
- (4) Nygren, M. A.; Pettersson, L. G. M.; Freitag, A.; Staemmler, V.; Gay, D. H.; Rohl, A. L. *J. Phys. Chem.* **1996**, *100*, 294.
- (5) Nygren, M. A.; Pettersson, L. G. M. *J. Phys. Chem.* **1995**, *99*.
- (6) Duke, C. B.; Meyer, R. J.; Paton, A.; Mark, P. *Phys. Rev. B* **1978**, *18*, 4225.
- (7) Ivanov, I.; Pollmann, J. *Phys. Rev. B* **1981**, *24*, 7275.
- (8) Wang, Y. R.; Duke, C. B. *Surf. Sci.* **1987**, *192*, 309.
- (9) Jaffe, J. E.; Harrison, N. M.; Hess, A. C. *Phys. Rev. B* **1994**, *49*, 11153.
- (10) Chang, S.-C.; Mark, P. *Surf. Sci.* **1974**, *46*, 293.
- (11) Duke, C. B.; Lubinsky, A. R. *Surf. Sci.* **1975**, *50*, 605.
- (12) Sambì, M.; Granozzi, G.; Rizzi, G. A.; Casarin, M.; Tondello, E. *Surf. Sci.* **1994**, *319*, 149.
- (13) Møller, P. J.; Komolov, S. A.; Lazneva, E. F. *Surf. Sci.* **1994**, *307*–*309*, 1177.
- (14) Thibado, P. M.; Rohrer, G. S.; Bonnell, D. A. *Surf. Sci.* **1994**, *318*, 379.
- (15) Ghiotti, G.; Chiorino, A.; Bocuzzi, F. *Surf. Sci.* **1993**, *287*, 228.
- (16) Jen, S. F.; Anderson, A. B. *Surf. Sci.* **1989**, *223*, 119.
- (17) Zhanpeisov, N. U.; Zhidomirov, G. M.; Baerns, M. *Zh. Strukt. Khim.* **1994**, *35*, 12.
- (18) Freitag, A. Ab initio Cluster-Rechnungen zur Untersuchung polarer Oberflächen von Übergangsmetalloxiden. PhD thesis, Ruhr-Universität Bochum, 1995.
- (19) Nakatsuji, H.; Fukunishi, Y. *Int. J. Quantum Chem.* **1994**, *42*, 1101.
- (20) Casarin, M.; Tondello, E.; Vittadini, A. *Surf. Sci.* **1994**, *303*, 125.
- (21) Casarin, M.; Tondello, E.; Vittadini, A. *Surf. Sci.* **1994**, *307*–*309*, 1182.
- (22) Gay, D. H.; Rohl, A. L. *J. Chem. Soc., Faraday Trans.* **1995**, *91*, 925.
- (23) Lewis, G. V.; Catlow, C. R. A. *J. Phys. C: Solid State Phys.* **1985**, *18*, 1149.
- (24) General Utility Lattice Program (GULP), developed by J.D. Gale, Royal Institution of Great Britain/Imperial College, 1992–5.
- (25) Schulz, H.; Thiemann, K. H. *Solid State Commun.* **1979**, *32*, 783.
- (26) Wyckoff, R. W. G. *Crystal Structures*; Wiley: New York, 1963.
- (27) Barandiarán, Z.; Seijo, L. *J. Chem. Phys.* **1988**, *89*, 5739.
- (28) Barandiarán, Z.; Seijo, L. newblock In *Studies in Physical and Theoretical Chemistry: Vol. 77(B), Computational Chemistry: Structure, Interactions and Reactivity*; Fraga, S., Ed.; Elsevier: Amsterdam, 1992; p 435.
- (29) Seijo, L. Private communication.
- (30) Ewald, P. P. *Ann. Phys.* **1921**, *64*, 253.
- (31) Parry, D. E. *Surf. Sci.* **1975**, *49*, 433.
- (32) Parry, D. E. *Surf. Sci.* **1976**, *54*, 195.
- (33) ECPAIMP is an integral program for ECP and AIMP calculations written by L.G.M. Pettersson, L. Seijo, and M. A. Nygren.
- (34) Nygren, M. A.; Pettersson, L. G. M.; Barandiarán, Z.; Seijo, L. *J. Chem. Phys.* **1994**, *100*, 2010.
- (35) Chong, D. P.; Langhoff, S. R. *J. Chem. Phys.* **1986**, *84*, 5606.
- (36) Wachters, A. J. H. *J. Chem. Phys.* **1970**, *52*, 1033.
- (37) Huzinaga, S. *J. Chem. Phys.* **1965**, *42*, 1293.
- (38) Cheng, W. H.; Kung, H. H. *Surf. Sci.* **1982**, *122*, 21.
- (39) Fripiat, J. G.; Lucas, A. A.; André, J. M.; Derouane, E. G. *Chem. Phys.* **1977**, *21*, 101.
- (40) Duke, C. B.; Lubinsky, A. R.; Chang, S. C.; Lee, B. W.; Mark, P. *Phys. Rev. B* **1977**, *15*, 4865.
- (41) Cappus, D.; Xu, C.; Ehrlich, D.; Dillmann, B.; Ventrice, C. A., Jr.; Shamery, A.; Kühlenbeck, K. H.; Freund, H.-J. *Chem. Phys.* **1993**, *177*, 533.
- (42) Refson, K.; Wogelius, R. A.; Fraser, D. G.; Payne, M. C.; Lee, M. H.; Milman, V. *Phys. Rev. Lett.* **1996**, *52*, 10823.
- (43) Huber, K. P.; Herzberg, G. *Molecular Spectra and Molecular Structure*; Van Nostrand Reinhold: New York, 1979.
- (44) Boussard, P.; Siegbahn, P. E. M.; Wahlgren, U. In *Adsorption on Ordered Surfaces of Ionic Solids and Thin Films: Springer Series in Surface Sciences, Vol. 33*; Freund, H.-H., Umbach, E., Eds.; Springer-Verlag: Berlin Heidelberg, 1993; p 192.
- (45) Anchell, J. L.; Morokuma, K.; Hess, A. C. *J. Chem. Phys.* **1993**, *99*, 6004.
- (46) Nygren, M. A.; Pettersson, L. G. M. *Chem. Phys. Lett.* **1994**, *230*, 456.
- (47) Pacchioni, G.; Ricart, J. M.; Illas, F. *J. Am. Chem. Soc.* **1994**, *116*, 10152.

JP953704H